Hypothesis

A model of a transmembrane drug-efflux pump from Gram-negative bacteria

Juan Fernandez-Recio, Fabien Walas, Luca Federici, J. Venkatesh Pratap, Vassiliy N. Bavro, Ricardo Nunez Miguel, Kenji Mizuguchi, Ben Luisi*

Department of Biochemistry, University of Cambridge, 80 Tennis Court Road, Cambridge CB2 1GA, UK

Received 24 September 2004; accepted 28 October 2004

Available online 18 November 2004

Edited by Takashi Gojobori

Abstract In Gram-negative bacteria, drug resistance is due in part to the activity of transmembrane efflux-pumps, which are composed of three types of proteins. A representative pump from *Escherichia coli* is an assembly of the trimeric outer-membrane protein TolC, which is an allosteric channel, the trimeric inner-membrane proton-antiporter AcrB, and the periplasmic protein, AcrA. The pump displaces drugs vectorially from the bacterium using proton electrochemical force. Crystal structures are available for TolC and AcrB from *E. coli*, and for the AcrA homologue MexA from *Pseudomonas aeruginosa*. Based on homology modelling and molecular docking, we show how AcrA, AcrB and TolC might assemble to form a tripartite pump, and how allostery may occur during transport.

Keywords: Pump-channel; Multidrug resistance; Transmembrane transport; Homology modelling; Molecular docking and allostery

1. Introduction

The therapeutic treatment of bacterial infection is frustrated frequently by the ability of the pathogen to acquire drug resistance. Such resistance is often caused by the activity of transmembrane transporters that recognize and expel efficiently from the cells a broad range of structurally unrelated cytotoxic drugs and xenobiotic compounds [1,2]. In the case of Gram-negative bacteria, which are characterized by a protective double-membrane system, an important group of drug efflux pumps is based on a tri-partite assembly, which is composed of an outer-membrane (OM) protein, an inner-membrane (IM) proton antiporter and a periplasmic membrane fusion protein (MFP) that links all these components [3–5]. These pumps transduce electrochemical energy to displace the drugs directionally.

*Corresponding author. Fax: +44 1223 766 002.
E-mail address: ben@cryst.bioc.cam.ac.uk (B. Luisi).

Abbreviations: OM, outer-membrane; IM, inner-membrane; MFP, membrane fusion protein; RND, resistance-nodulation-division; MFS, major facilitator superfamily

A representative pump that expels acridine and other compounds from *Escherichia coli* is shown schematically in Fig. 1(a). The TolC protein of this pump is a representative member of the OM family of efflux pump components. In *E. coli*, TolC has the ability to interact with different classes of IM proton antiporters, which may belong either to the resistance nodulation and cell division family (RND) or to the major facilitator superfamily (MFS) [6,7]. A typical drug efflux pump observed in *E. coli* is formed by the RND protein AcrB [8,9], the MFP AcrA, and the OM channel TolC [10,11]. Insight into the mechanism of multidrug transport has been attained with the determination of the crystal structures of TolC [12], AcrB [8,13] and more recently MexA, a MFP from *Pseudomonas aeruginosa* that is a close homologue to AcrA [14,15] (see Fig. 1 for a gallery of these components). TolC and AcrB both form homotrimers, and both contain sealed channels that are likely to be opened during the transport process.

The question remains as to how these three proteins assemble to form a functional pump and how channel opening occurs. Here, we have explored the possible interactions between TolC, AcrB and AcrA by homology modelling and molecular docking. We propose a structural model for the tripartite complex, where the TolC channel is stabilized in an open conformation state by interacting with the coiled-coil domain of AcrA, which in turn interacts with the IM protein AcrB to bridge the IM and OM proteins. This model may explain transport through homologous pumps amongst the Gram-negative bacteria.

2. A homology model of AcrA

The crystal structure of MexA reveals an intricate fold that is a composite of structural domains found widely in nature. As successfully predicted by Johnson and Church [16], the core of this MFP has structural similarity with the "lipoyl/biotinyl" domain, which occurs in the extensive family of proteins that are modified by a lipoyl group or biotin. Emanating from the lipoyl/biotinyl domain, there is a pair of α-helices that form a classical coiled-coil, with the characteristic knobs-into-holes intermeshing of hydrophobic residues. This internal interface is structurally invariant amongst the 13 copies of MexA that occupy the crystallographic asymmetric unit in non-equivalent packing environments, and it is unlikely to undergo any type of plastic deformation on engagement with the other

0014-5793/$22.00
doi:10.1016/j.febslet.2004.10.097

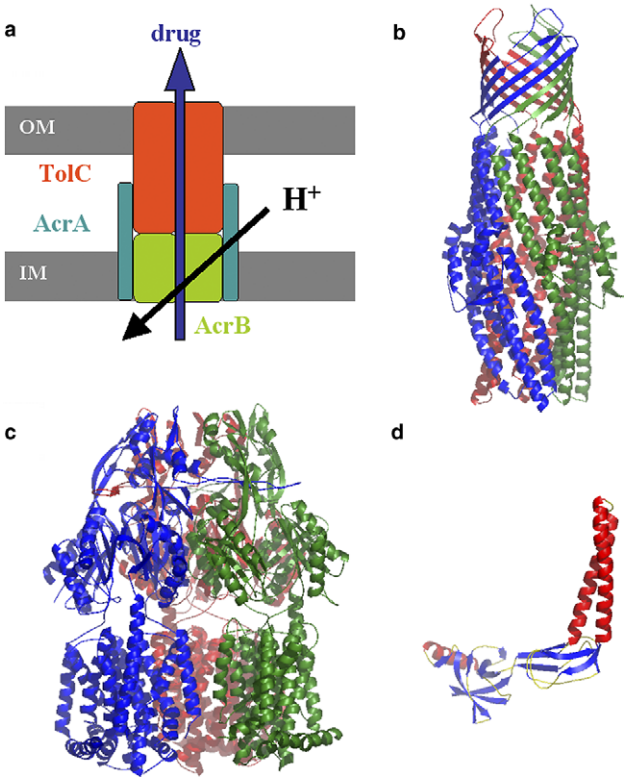

Fig. 1. Efflux pumps from Gram-negative bacteria. (a) A schematic representation of the assembly of the acridine-efflux pump from *E. coli*. Also shown are the crystal structures of representative components of bacterial efflux pumps: (b) the *E. coli* OM protein TolC, a homotrimer; (c) the trimeric *E. coli* AcrB IM protein, and (d) the *Pseudomonas aeruginosa* MexA MFP. The AcrB and TolC molecules are orientated with the molecular threefold axes orientated vertically.

components of the pump. All known members of the family conserve the core of the lipoyl/biotinyl domain as well as the coiled-coil; however, the length of the coiled-coil is variable – a point that will become important later in the analysis of the docking model. The coiled-coil region of AcrA is predicted to be 14 residues longer than the one in MexA, and based on the assumption that this region will make an elongated coiled-coil, a model of AcrA was created (details in Fig. 2 legend).

3. The open state of TolC and the docking of AcrA

Like AcrB, the TolC protein is a homotrimer. Also, in both proteins it appears that the subunit originated through a gene duplication event, which has left a signature as a recognizable structural repeat within the protomer. The TolC open state was modelled on the basis of this structural repeat, by simply assuming that the coiled-coil portion of the two halves has quasi-equivalent super-helical geometry [17]. On comparing the open and closed states, we were struck by the appearance of an exposed groove at the interface of the subunits that occurs at the boundary of adjacent coiled-coils (Fig. 2(b)). We found that this groove could easily accommodate an α-helix with a gentle super-helical trajectory [18]. The docked helix can form contacts with the exposed helices of TolC to form, locally, a helical bundle. Based on this observation, we manually docked the AcrA model into the open state of TolC. A total of eight different possible docking orientations of AcrA with respect to TolC were obtained with this manual procedure. These AcrA/TolC docking complexes were further refined using a procedure for optimization of interface side-chain conformation (ICM-DISCO; [19,20]). We found an optimal local energy minimum, with scoring energy of −40.5 kcal/mol (Table 1), which forms close interfacial contacts (Fig. 2(c)). Three such interfacial grooves are present in the TolC trimer, and so three AcrA protomers can be accommodated. Two other docking orientations (ranked second and third in Table 1) were considered for further modelling. The conformation ranked number four, although it had only slightly less favourable value for the scoring-energy, was not considered for further modelling because it occluded the bottom of the TolC channel. The scoring energy used here to evaluate the docking results represents the balanced sum of contributions from the van der Waals, electrostatics, hydrogen bonding and desolvation binding energies, which have been optimized with datasets of known protein–protein complexes [19,21]. This model represents the first part of the tripartite pump.

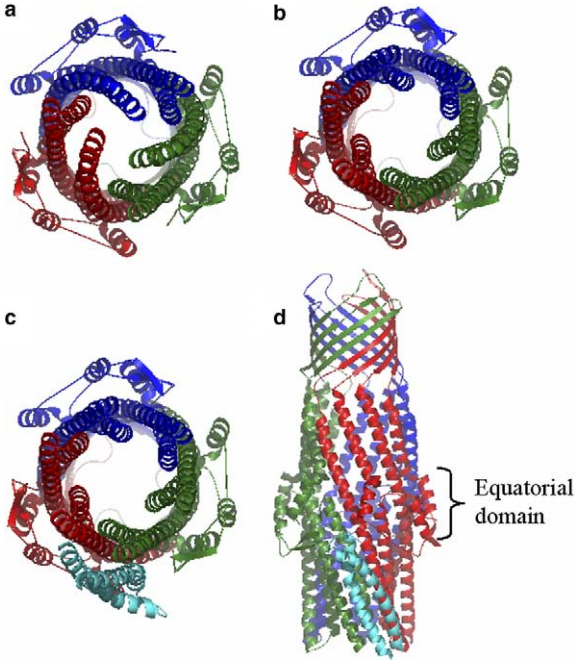

Fig. 2. A comparison of the closed (resting) and open states of TolC and the docking of AcrA. The views in part a, b, and c show the aperture end of TolC, from the perspective of the IM partner protein. Presented here are the closed state, from the crystal structure (a); the open state, as modelled on the internal molecular symmetry (b); the open state with the coiled-coil domain from AcrA docked in the inter-protomer interface (c). In (d), the TolC–AcrA complex has been rotated so that the molecular threefold axis is vertical. AcrA was prepared by homology modelling.

4. Docking of TolC and AcrA onto the AcrB trimer

We analyzed the surface of TolC for sites that are likely to interact with other proteins, using a method that finds Optimal Docking Areas (ODAs), i.e. regions with optimal desolvation energy for protein binding [22]. In general, ODAs with values smaller than −15.0 kcal/mol are more than 80% likely to be

Table 1
Results of the different docking/refinement runs

TolC/AcrA			TolC/AcrB			TolC/AcrB/AcrA[a]			TolC/AcrB/AcrA[b]		
Rank	Energy (kcal/mol)	RMSD[c] (Å)	Rank	Energy (kcal/mol)	RMSD[c] (Å)	Rank	Energy (kcal/mol)	RMSD[d] (Å)	Rank	Energy (kcal/mol)	RMSD[d] (Å)
1	−40.5	0.0	1	−45.4	0.0	1	−77.0	0.0	1	−82.6	0.0
2	−34.1	5.4	2	−42.8	16.1	2	−74.3	5.6	2	−82.4	4.3
3	−33.6	6.3	3	−29.6	16.4	3	−72.9	9.9			
4	−33.0	22.5	4	−28.2	15.9	4	−72.8	8.3			
5	−26.2	24.1	5	−18.8	13.4	5	−72.7	4.8			
6	−22.6	8.4	6	−10.0	9.9	6	−69.9	6.2			
7	−19.9	22.2									
8	−14.1	24.2									

[a] Refinement of TolC/AcrA docking solutions 1–3 combined with TolC/AcrB docking solutions 1 and 2.
[b] Refinement of AcrA final model with TolC/AcrB docking solutions 1 and 2. See text for details.
[c] RMSD calculated for the interface (4 Å from receptor) ligand Cα atoms when TolC molecules are superimposed. Values referred to the lowest-energy docking solution.
[d] RMSD calculated for the interface (4 Å from receptor) AcrA Cα atoms when TolC/AcrB molecules are superimposed. Values referred to the lowest-energy docking solution.

correctly located in protein–protein binding interfaces, as it has been previously determined in a large data set of known protein–protein complexes. In both the open and closed states of TolC, the portions with greatest propensity for interaction, with values of up to −26.4 and −33.6 kcal/mol for open and closed states, respectively, are the inter-helical loops near the aperture (the bottom portion shown in Fig. 1(b)). This region is not predicted to interact with AcrA according to our model, but it can potentially match to the funnel shaped surface of the periplasmic domain of AcrB (Fig. 1(c)). The direct intermeshing of TolC with AcrB has been proposed by Murakami et al. [8], whereby the inter-helical loops of TolC meet the surface concavity present in AcrB. In this model, the threefold molecular symmetry axes of TolC and AcrB are coincident.

We explored and refined a more detailed model for the direct docking of AcrB with the open state TolC. To proceed, we first noted that both the TolC and AcrB trimers expose six inter-helical loops for potential contact; these arise from the approximate structural repeat within the protomer that we described earlier. As these protrusions all lie in a ring, they form the shape of a six-pointed crown. We sought the global energy minimum of the interaction between the open state of TolC and AcrB by performing an unrestricted rigid-body 2-dimensional search of rotations around the coincident threefold symmetry axes and translation along this axis. The rigid-body conformational search and subsequent interface side-chain refinement were performed as previously described [19,20]. We found two major minima in which TolC and AcrB were intermeshed in two non-equivalent ways (scoring energies −45.4 and −42.8 kcal/mol, respectively). The lower energy solution is shown in Fig. 3(a); the second one was not chosen for further refinement because it caused a steric clash of AcrA with the AcrB in the next stages of modelling (see below). The remaining docking orientations were clearly less favourable energetically (Table 1). For comparison, we have docked the closed conformation of TolC onto AcrB, but the resulting conformations, equivalent to the ones obtained for the open TolC/AcrB docking, had less favourable energy values (−36.1 and −29.3 kcal/mol, respectively).

We refined the three selected models described in the previous section for AcrA/TolC interaction, in the context of the two possible modes of TolC/AcrB interaction described above. However, the resulting solutions were not yet optimal, in spite of their reasonable energy values, because of the fact that AcrA backbone was initially considered rigid, as explained below. It is interesting to note that the AcrB trimer has a striking canyon-like groove along the interface of the entire periplasmic domain. With the constraint that the AcrA coiled-coil tracks along the TolC groove, the lipoyl/biotinyl domain exits the TolC in the vicinity of this AcrB interfacial groove. This domain can be accommodated into the AcrB groove, but not simultaneously with the fit of the coiled-coil domain in the TolC groove, when the AcrA backbone is rigid.

However, with a modest structural adjustment, the AcrA can engage both grooves simultaneously. The connecting region between the coiled-coil and lipoyl/biotinyl domains is thus predicted to act as a conformational switch. The putative switch provides an explanation for the observed phenotypes of several previously described MexA mutations which are located in this region and have been shown to impede MexA–MexB association and MexA self-association [23].

We suggest that the lipoyl/biotinyl domain would be accommodated in the intra-subunit gap of AcrB, with slight conformational strain, to form a closed seal between TolC, AcrA and AcrB. We built a TolC/AcrB/AcrA model by superimposing the AcrA coiled-coil domain onto the best solution obtained from the TolC/AcrA docking (described before; see Fig. 2(c)) and the AcrA lipoyl/biotinyl domain onto a selected solution of the TolC/AcrB/AcrA refinement, where the lipoyl/biotinyl domain had good interface complementarity to AcrB. This was performed for each of the two possible TolC/AcrB orientations, and the final energy values obtained for the refined complex models were −82.6 and −82.4 kcal/mol, respectively, better than when AcrA was considered as a rigid-body. This energy value accounts not only for the binding of AcrA onto the TolC/AcrB complex, but also for the previous binding of TolC onto AcrB. Our final lowest-energy model, incorporating the required match of TolC and AcrB and the accommodation of AcrA into the interfacial grooves of both its partners, is shown in Fig. 3(b). When we used the closed form of TolC, we obtained less favourable energy values for the final models in which AcrA was bound onto the two possible closed TolC/AcrB orientations (−75.2 and −69.2 kcal/mol, respectively).

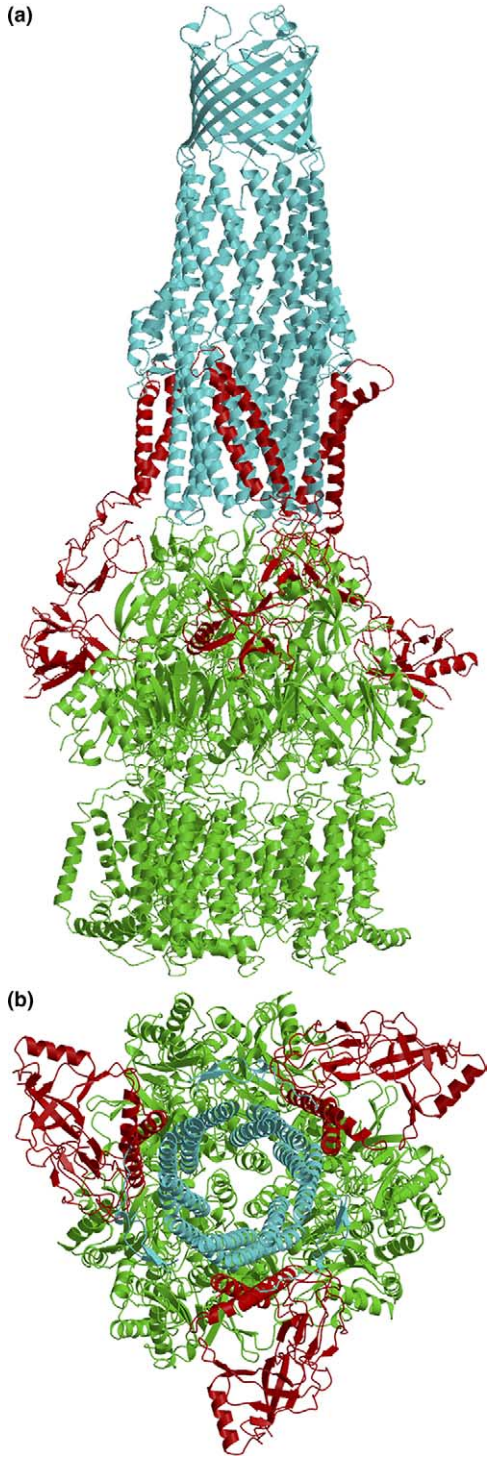

Fig. 3. Two views of the AcrA–AcrB–TolC assembly. In (a), the threefold molecular axis is vertical, and in (b), the view is along the threefold axis. AcrA is predicted to fit simultaneously in the inter-protomer grooves of TolC and AcrB, with conformational strain. Initially, AcrA best model was docked manually onto the TolC structure using Insight II software (Accelrys). We placed 2 models of AcrA by positioning its coiled-coil domain such that it forms a helical bundle with the two helices of TolC. The 3D coordinates for this TolC/AcrA complex were submitted to a rigid body simulation-docking program based on multi-start global energy optimization of an all-atom model of AcrA. The ensembles of the rigid-body docking solutions generated by the simulations were subsequently used to project the docking energy landscapes onto the protein surface.

This indicates that the open conformation of TolC may bind more strongly to AcrB and AcrA than the closed one.

Our model can account for the effects of mutations in the homologous MexA that abolish MexA–MexB association, but which do not impede self-association of the protein. These mutations map to the lipoyl/biotinyl domain and lie in close vicinity of the AcrB surface [23]. Some of these, notably L301 and R294, are inferred by our model to be in direct contact with the AcrB. Our model also provides a rationalization of the experimental data of Touze and Eswaran [24], showing that truncation of the N-terminal portion of AcrA abolishes binding to TolC but not to AcrB.

5. Methods

After searching for the best template with the web-based programs FUGUE and HOMSTRAD [25–28], 3D homology models of AcrA were built with the template crystal structures of MexA (PDB entry 1vf7). The alignments were performed with FUGUE and annotated with JOY [29]. After examinations of the alignments, 15 models were generated using MODELLER [30] and these were ranked by analysis of their stereochemistry using PROCHECK [31] and their sequence–environment compatibility using VERIFY 3D [32,33]. From the ensemble, the highest-ranking structure on the basis of these criteria was selected for further analysis and as a starting structure for docking simulations. All figures have been prepared using the programs MOLSCRIPT [34] and rendered using Raster3D [35].

6. Conclusions and discussion

To date, there is no definitive experimental data for the stoichiometric composition of an engaged transport pump. The model we have prepared predicts a protomer stoichiometry of 1:1:1 for OM:MFP:IM components of the tripartite pump. An alternative model for the pump has also been suggested based on the compositional ratio of 1:3:1 and this requires that the MFP forms an enclosing sheath around the TolC [15]. A model of 1:2:1 has also been proposed in which the helices of the coiled-coil are inclined with the surface of TolC and do not fit into the inter-subunit grooves [14]. Our model differs from both in that it predicts the alignment of the coiled-coil of the MFP within a groove with shape complementarity in the open state of TolC, and it also predicts the direct interaction of OM and IM components, which is not possible in the models of Akama et al. [14] and Higgins et al. [15]. We note that while the proposed model is applicable for the AcrA–AcrB–TolC system, different arrangement of the MFPs can be expected in ABC and MFS-based pumps. Thus, in the haemolysin transporter, which uses an IM ATPase, the MFP component may form a closed tube [17], like that proposed by Higgins et al. [15] for MexA.

Experimental evidence suggests that TolC can be found in isolation from the other pump components and this implies that it must be in the closed, resting state; otherwise it would provide a large open pore in the OM. The allosteric transition in TolC to its open state is likely to be favoured by interactions with the other components of the tripartite pumps and we have shown here how the grooves of the open state of TolC can be matched favourably by the MFP partner. We also propose that, with a structural adjustment, the lipoyl/biotinyl domain of AcrA will dock into clefts in the periplasmic surface of the AcrB trimer to form the tripartite pump. In our model,

the AcrB pore is closed, and the question arises as to how it is opened during the transport process. The crystal structure of AcrB in complex with drugs shows that these ligands do not trigger the opening of the periplasmic pore, and it therefore seems likely that pore opening may require the binding of drug, the conduction of protons and the protein–protein interactions with TolC and AcrA. Thus, the simultaneous engagement of the MFP with the IM and OM, and the allosteric transitions triggered through drug binding and proton conduction, may ensure the orchestrated opening of the IM pore and the vectorial transport of drug.

Acknowledgement: This work was supported by the Wellcome Trust. L.F. and J.F-R. are recipients of Marie Curie fellowships. We thank Chris Calladine and Matthew Higgins for helpful discussions.

References

[1] Li, X.Z. and Nikaido, H. (2004) Efflux-mediated drug resistance in bacteria. Drugs 64 (2), 159–204.
[2] McKeegan, K.S. and Borges-Walmsley, M.I., et al. (2004) Curr. Opin. Pharmacol. 4, 479–486.
[3] Zgurskaya, H.I. and Nikaido, H. (2000) Multidrug resistance mechanisms: drug efflux across two membranes. Mol. Microbiol. 37 (2), 219–225.
[4] Zgurskaya, H.I. and Nikaido, H. (2000) Cross-linked complex between oligomeric periplasmic lipoprotein AcrA and the inner-membrane-associated multidrug efflux pump AcrB from *Escherichia coli*. J. Bacteriol. 182 (15), 4264–4267.
[5] Poole, K. (2004) Efflux-mediated multiresistance in Gram-negative bacteria. Clin. Microbiol. Infect. 10 (1), 12–26.
[6] Paulsen, I.T. and Brown, M., et al. (1996) Proton-dependent multidrug efflux systems. Microbiol. Rev. 60 (4), 575–608.
[7] Lomovskaya, O. and Zgurskaya, H.I., et al. (2002) It takes three to tango. Nat. Biotechnol. 20 (12), 1210–1212.
[8] Murakami, S. and Nakashima, R., et al. (2002) Crystal structure of bacterial multidrug efflux transporter AcrB. Nature 419 (6907), 587–593.
[9] Yu, E.W. and McDermott, G., et al. (2003) Structural basis of multiple drug-binding capacity of the AcrB multidrug efflux pump. Science 300 (5621), 976–980.
[10] Nikaido, H. and Zgurskaya, H.I. (2001) AcrAB and related multidrug efflux pumps of *Escherichia coli*. J. Mol. Microbiol. Biotechnol. 3 (2), 215–218.
[11] Tikhonova, E.B. and Zgurskaya, H.I. (2004) AcrA, AcrB and TolC of *Escherichia coli* form a stable intermembrane multidrug efflux complex. J. Biol. Chem. 279 (31), 32116–32124.
[12] Koronakis, V. and Sharff, A., et al. (2000) Crystal structure of the bacterial membrane protein TolC central to multidrug efflux and protein export. Nature 405 (6789), 914–919.
[13] Pos, K.M. and Schiefner, A., et al. (2004) Crystallographic analysis of AcrB. FEBS Lett. 564 (3), 333–339.
[14] Akama, H. and Matsuura, T., et al. (2004) Crystal structure of the membrane fusion protein, MexA of the multidrug transporter in *Pseudomonas aeruginosa*. J. Biol. Chem. 279 (25), 25939–25942.
[15] Higgins, M.K. and Bokma, E., et al. (2004) Structure of the periplasmic component of a bacterial drug efflux pump. Proc. Natl. Am. Sci. 101 (27), 9994–9999.
[16] Johnson, J.M. and Church, G.M. (1999) Alignment and structure prediction of divergent protein families: periplasmic and outer membrane proteins of bacterial efflux pumps. J. Mol. Biol. 287 (3), 695–715.
[17] Sharff, A. and Fanutti, C., et al. (2001) The role of the TolC family in protein transport and multidrug efflux. From stereochemical certainty to mechanistic hypothesis. Eur. J. Biochem. 268 (19), 5011–5026.
[18] Federici, L. and Walas, F., et al. (2004) The structure and mechanism of the TolC outer membrane transport protein. Curr. Sci. 86 (12), 25–30.
[19] Fernández-Recio, J. and Totrov, M., et al. (2002) Soft protein–protein docking in internal coordinates. Protein Sci. 11, 280–291.
[20] Fernández-Recio, J. and Totrov, M., et al. (2003) ICM-DISCO Docking by global energy optimization with fully flexible side-chains. Proteins 52, 113–117.
[21] Fernández-Recio, J. and Totrov, M., et al. (2004) Identification of protein–protein interaction sites from docking energy landscapes. J. Mol. Biol. 335, 843–865.
[22] Fernández-Recio, J., Totrov, M., et al. (2004) ODA (Optimal Desolvation Area): a new method for predicting protein–protein interaction sites. Proteins (in press).
[23] Nehme, D. and Xian-Zhi, L., et al. (2004) Assembly of the MexAB-OprM multidrug efflux system of *Pseudomonas aeruginosa*: identification and characterization of mutations in mexA compromising MexA multimerization and interaction with MexB. J. Bacteriol. 186 (10), 2973–2983.
[24] Touze, T. and Eswaran, J., et al. (2004) Interactions underlying assembly of the *Escherichia coli* AcrAB-TolC multidrug efflux system. Mol. Microbiol. 53, 697–706.
[25] Mizuguchi, K. and Deane, C.M., et al. (1998) HOMSTRAD: a database of protein structure alignments for homologous families. Protein Sci. 7 (11), 2469–2471.
[26] Shi, J. and Blundell, T.L., et al. (2001) FUGUE: sequence–structure homology recognition using environment-specific substitution tables and structure-dependent gap penalties. J. Mol. Biol. 310 (1), 243–257.
[27] Williams, M.G. and Shirai, H., et al. (2001) Sequence–structure homology recognition by iterative alignment refinement and comparative modeling. Proteins Suppl. 5, 92–97.
[28] Stebbings, L.A., Mizuguchi, K. (2004) HOMSTRAD: recent developments of the Homologous Protein Structure Alignment Database. Nucleic Acids Res. 32 Database issue, D203–7.
[29] Mizuguchi, K. and Deane, C.M., et al. (1998) JOY: protein sequence–structure representation and analysis. Bioinformatics 14 (7), 617–623.
[30] Fiser, A. and Sali, A. (2003) Modeller: generation and refinement of homology-based protein structure models. Methods Enzymol. 374, 461–491.
[31] Laskowski, R.A. and MacArthur, M.W., et al. (1993) PROCHECK: a program to check the stereochemical quality of protein structures. J. Appl. Crystallogr. 26, 283–291.
[32] Luthy, R. and Bowie, J.U., et al. (1992) Assessment of protein models with threedimensional profiles. Nature 356 (6364), 83–85.
[33] Eisenberg, D. and Luthy, R., et al. (1997) VERIFY3D: assessment of protein models with three-dimensional profiles. Methods Enzymol 277, 396–404.
[34] Kraulius, P.J. (1991) MOLSCRIPT: a program to produce both detailed and schematic plots of protein structures. J. Appl. Crystallogr. 24, 946–950.
[35] Merritt, E.A. and Bacon, D.J. (1997) Raster3D: Photorealistic molecular graphics. Methods Enzymol. 277, 505–524.